Electronic structure of cubic and tetragonal zirconia

Henri J. F. Jansen
Department of Physics, Oregon State University, Corvallis, Oregon 97331-6507
(Received 24 August 1990)

The electronic structure of tetragonal zirconia with D_{4h}^{15} symmetry is investigated using density-functional theory. The Kohn-Sham equations are solved by applying the full-potential linearized augmented-plane-wave method. The total energy as a function of the lattice parameters shows that at zero temperature tetragonal zirconia is more stable than cubic zirconia. The calculated elastic constants are consistent with experimental data. High-temperature results are simulated by introducing a semiempirical volume expansion. The calculated displacement in the positions of the oxygen atoms follows the experimental results, but the tetragonal distortion as a function of temperature shows larger differences with experiment. At expanded volumes the tetragonal structure is always more stable than the cubic structure, but the energy differences are of the same order of magnitude as the thermal energies.

I. INTRODUCTION

Zirconia (ZrO_2) is a very important ceramic material. Its applications include the use in extrusion dies, oxygen sensors, and artificial diamonds. Zirconia was discovered as baddeleyite in 1892 by Hussak. Nernst[1] was probably the first to investigate and report on the properties of zirconia. One problem in the applications of zirconia as a ceramic material is a monoclinic-to-tetragonal phase transition[2] which occurs at 1170 °C. The low-temperature monoclinic form has a larger volume than the tetragonal modification and a very anisotropic thermal expansion. Samples made at high temperature often fall apart when they are cooled below this transition temperature. A second transition occurs around 2370 °C. Above this temperature zirconia has a simple-cubic CaF_2 structure. This cubic structure can be stabilized at lower temperatures by adding dopants like Y_2O_3. The melting point of zirconia is 2680 °C.

The nature of the phase transitions in zirconia is not well understood from a theoretical point of view. There are many questions pertaining to the low-temperature monoclinic-to-tetragonal phase transition. The number of atoms in the unit cell of monoclinic zirconia is twelve, and hence electronic structure calculations for this modification are quite involved. Although our ultimate goal is to investigate the monoclinic-to-tetragonal phase transition, we have decided to first study the high-temperature tetragonal-to-cubic transition because it is easier to study theoretically. In this paper we present the results of our *ab initio* electronic structure calculations for tetragonal zirconia. We consider cubic zirconia to be a special case of this structure and hence results for the fluorite structure are included in this paper. Figure 1 shows the unit cell used in this work. The external parameters describing the unit cell are a and c. For the ideal CaF_2 structure $c/a=\sqrt{2}$. In tetragonal zirconia there is an internal displacement of the oxygen atoms along the z direction. Alternating columns of oxygen atoms are shifted upwards and downwards by an amount Δc. The third, internal, parameter describing the tetragonal unit cell is d_z and is related to this displacement of the oxygen atoms by $d_z=\Delta c/c$.

Due to the complex nature of the crystal structure of zirconia, there are not many previous calculations. Early investigations used simple chemical arguments to explain the stability of monoclinic zirconia.[3] A cluster calculation[4] showed the effect of changes in the electron levels as a function of structure. To our knowledge, the first *ab initio* results for zirconia were published by Boyer and Klein.[5] These authors used a combination of a band-structure and a pair-potential approach to obtain the elastic and thermal properties of cubic zirconia. They found that the cubic fluorite structure has the lowest energy, but that at expanded volumes the tetragonal structure is relatively more stable. Later results were presented at the International Conference on Electronic Structure and Phase Stability in Advanced Ceramics[6] in 1987, where we also presented preliminary data.[7]

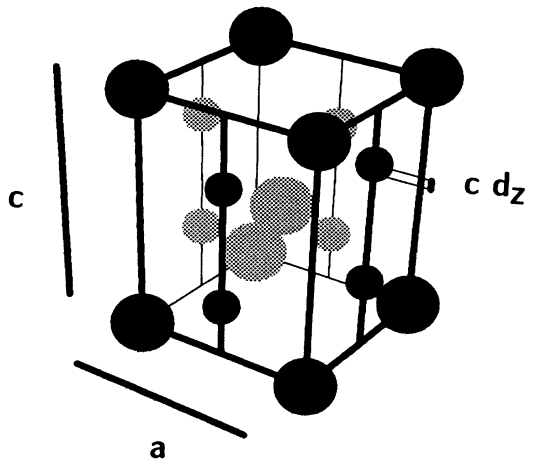

FIG. 1. Unit cell of tetragonal zirconia.

II. METHODS

Electronic structure calculations for large systems are most easily performed within the framework of the density-functional theory.[8] This theory provides a prescription to obtain the total electronic energy of a solid as a function of the geometry of the atoms. The equilibrium structure is found by minimizing this total energy, while elastic constants are related to the curvature of the total-energy surface at the equilibrium configuration. The charge density evaluated via density-functional calculations is a true representation of the charge density of the electronic system, but the energy bands are only first-order approximations to the excitation energies of the electrons.

The total energy as a functional of the charge density $\rho(\mathbf{r})$ in density-functional theory is expanded as a sum of four terms. Easy to calculate are (i) the classical Coulomb energy pertaining to the charge density $\rho(\mathbf{r})$, (ii) the external energy due to the Coulomb forces of the nuclei, and (iii) the exchange-correlation energy. We use the local-density approximation for the exchange-correlation energy in the form due to von Barth and Hedin and parametrized by Janak.[9] This approximation of the many-body effects in the electronic system has given very good results for many simple metals, semiconductors, and transition metals.[10] The evaluation of the fourth term, the kinetic energy of a reference system of noninteracting particles with charge density $\rho(\mathbf{r})$ is very time consuming. The standard computational approach employs the Kohn-Sham equations.[8] In our case these Kohn-Sham equations are solved using the full-potential linearized augmented-plane-wave (FLAPW) method.[11] This precise, but slow, method is needed to obtain reliable results for structures with a low symmetry. Spherical approximations to the potential and charge density introduce errors which are probably too large.

III. CONVERGENCE TESTS

In the FLAPW method one divides space into two regions. Near the atoms all quantities of interest are expanded in spherical harmonics and in the interstitial region they are expanded in plane waves. The first type of expansion is defined within a so-called muffin-tin sphere of radius R_{MT} around each nucleus. In our calculations we have chosen $R_{MT}(0)=1.69$ a.u. and $R_{MT}(\mathrm{Zr})=2.00$ a.u. (1 a.u.$=0.0529$ nm). At first we used a larger value of R_{MT} for Zr and a smaller value for 0, but this gave numerical problems related to the Zr $4p$ electrons and the O $2s$ electrons.

In the FLAPW method one makes a distinction between core electrons and valence electrons. The eigenvalues of the core electrons are calculated using a fully relativistic equation of motion, excluding the nonspherical parts of the potential inside the muffin tins. The quantum states of the valence electrons are evaluated using band states and the full nonspherical potential, but with semirelativistic equations of motion. The latter approximation simplifies the numerical procedures dramatically. In zirconia, however, the omission of spin-orbit coupling is not important. In our work the O $2s$ and $2p$ electrons were treated as valence electrons as well as the Zr $4s$, $4p$, and up. Details are given in Table I. In the FLAPW method the charge density can be easily analyzed in terms of the l-decomposed total charge inside the muffin-tin spheres and the interstitial charge. Obviously, these numbers have no absolute meaning, since they depend on the choice of sphere radii. Changes in these numbers, however, do convey useful information pertaining to the response of the system. One also has to keep in mind that in a well-converged calculation the choice of these radii does not affect the value of the total energy.

We have used one energy window for all valence and semicore bands. The energy parameters for Zr $l=0$ and $l=1$ and for O $l=0$ were determined from the positions of the semicore electrons, while all the other energy parameters were set according to the average valence-band energy. A better procedure is to use separate energy windows for all these bands, since the lack of orthogonality between the bands does not seem to introduce large errors.[12] Fortunately, in our case the errors resulting from the use of one energy window are also small. They are mainly connected with the use of Zr $4p$ instead of $5p$ orbitals in describing the valence band. The total contribution of these electrons to the valence band is only 1%, and the change in this contribution as a function of the geometry is much smaller. This situation is very different from that encountered in bulk iron. In that case the amount of p character in the conduction band is about 5%, but important states are at the Fermi level and changes in the p character are large. In iron one does not

TABLE I. Energy bands and charge decomposition of semicore and valence electrons for $a=6.88$ a.u., $c=9.96$ a.u., and $d_z=0.065$. These values do not change much for other geometries.

	Zr $4s$	Zr $4p$	O $2s$	O $2p$
Average energy (Ry)	−2.94	−1.33	−0.60	0.39
Width at Γ (mRy)	5	36	116	338
Charges:				
Interstitial	0.19	1.39	1.24	6.80
Zr $4s$	3.80	0.00	0.03	0.07
Zr $4p$	0.00	10.26	0.39	0.31
Zr $4d$	0.00	0.00	0.08	1.48
O $2s$	0.00	0.24	6.24	0.10
O $2p$	0.01	0.09	0.01	15.14
Total	4.00	12.00	8.00	24.00

obtain good results using one energy window and including the $3p$ semicore electrons in the band structure.

Important tests for the precision of our results are the convergence as a function of the number of basis functions and k points used to solve the equations of motion for the equivalent system of noninteracting particles. These parameters determine the precision of the noninteracting kinetic energy and hence the total energy. Since zirconia is an insulator the number of k points in the Brillouin zone at which we solve the Kohn-Sham equations is not a sensitive parameter. The best approach would be to use special k points, since they are ideal for a situation where there are no discontinuities due to a Fermi surface. We have, however, simply used the standard tetrahedron scheme with 20 points in the irreducible part of the first Brillouin zone. This gives a relative precision much better than 1 mRy in our total-energy data. The number of basis functions is governed by a parameter $k_{\max}$, which is the radius of a sphere is a reciprocal space. Plane waves with reciprocal lattice vectors within this sphere are included in the set of basis functions. We have used $k_{\max}=4$, which corresponds to about 100 basis functions per atom in the calculations. The relative errors in our total-energy data due to the numerical constraints are about 1 mRy per unit cell. The errors due to basis-size limitations give the largest contribution to the relative error in the data.

IV. SYMMETRIC ZIRCONIA

As we have mentioned before, tetragonal zirconia is described by three structural parameters. The first two specify the size of the unit cell in the x and y direction, a, and in the z direction, c. The last parameter, d_z, describes the change in internal structure related to the oxygen atoms moving away from the ideal CaF_2 positions. Figure 1 shows these parameters and the unit cell we are using. We first focus on one aspect of the effects of changes in these structural parameters, and keep the oxygen atoms at their ideal positions. For convenience, we call this configuration symmetric zirconia. Actually, we have taken $d_z=0.01$, slightly away from the symmetric positions, in order to make a distinction between the two types of oxygen atoms. By doing so we avoid some numerical instabilities in the convergence of the calculations which sometimes show up in calculations at reduced symmetry for systems which actually have a higher symmetry. Our value of d_z is very small, however, and we can treat it as zero for all purposes.

Table II gives our total-energy data as a function of a and c for $d_z=0.01$. As we have discussed before, the relative error of these total-energy values is about 1 mRy, although the absolute error is larger. In Fig. 2 we show the data points in a different representation. The horizontal axis represents V, the volume of the unit cell scaled with respect to the experimental[13] volume of cubic (or tetragonal) zirconia extrapolated to zero temperature, $V_{\text{ref}}=444$ a. u. The vertical axis denotes r, the c/a ratio, and cubic zirconia corresponds to $r=\sqrt{2}=1.414$. The advantage of this representation is that for cubic systems a second-order expansion in these coordinates contains no cross terms: the data in that case fit to ellipses with their axes parallel to the coordinate system. The num-

TABLE II. Total-energy data. Calculated total energy per unit cell of symmetric zirconia as a function of the lattice parameters a and c (in a.u.). The ratio $r=c/a$ and the volume V is a^2c/V_{ref}, with $V_{\text{ref}}=444$ a.u. The total energy only gives the mRy part, the complete value is obtained by adding $-14\,980$ Ry to all data. Our unit cell contains six atoms.

a (a.u.)	c (a.u.)	V	r	E (mRy)
6.88	9.96	1.0623	1.4477	−206
6.91	9.89	1.0641	1.4313	−207
6.93	9.81	1.0616	1.4156	−209
6.95	9.73	1.0590	1.4000	−211
6.97	9.70	1.0618	1.3917	−207
6.84	9.96	1.0500	1.4561	−211
6.80	9.96	1.0377	1.4647	−217
6.76	9.96	1.0256	1.4734	−217
6.72	9.92	1.0094	1.4762	−221
6.68	9.88	0.9934	1.4790	−225
6.64	9.84	0.9776	1.4819	−223
6.68	9.80	0.9854	1.4671	−229
6.72	9.76	0.9931	1.4524	−230
6.76	9.72	1.0009	1.4379	−229
6.80	9.68	1.0086	1.4235	−228
6.70	9.70	0.9811	1.4478	−230
6.70	9.64	0.9751	1.4388	−230
6.70	9.58	0.9690	1.4299	−231
6.70	9.52	0.9629	1.4209	−230
6.70	9.46	0.9569	1.4119	−228
6.76	9.46	0.9741	1.3994	−232
6.82	9.46	0.9915	1.3871	−228
6.88	9.52	1.0154	1.3837	−224
6.88	9.58	1.0218	1.3924	−224

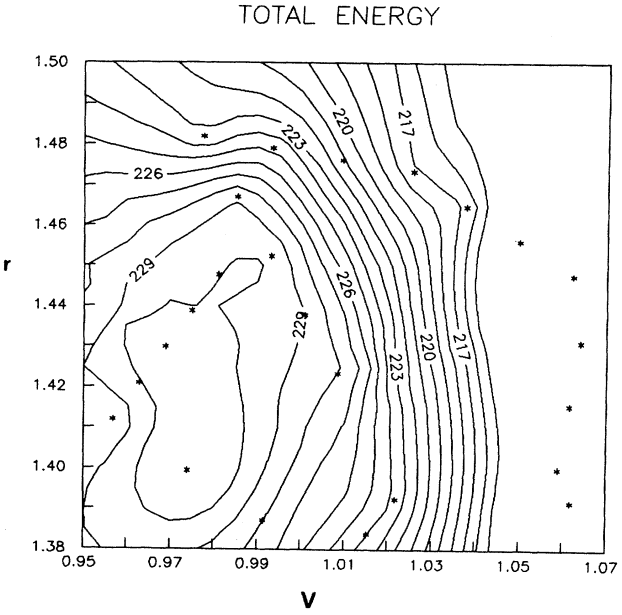

FIG. 2. Contours of equal total energy of tetragonal zirconia. Subsequent contour lines correspond to energy values which differ by 1 mRy. *Ab initio* data points are indicated by stars.

bers in this figure give the fractional part of the total energy and are in mRy; we omitted the minus sign in front of the total energy. The contour lines in Fig. 2 are obtained numerically by local fits to the data and only have a qualitative meaning.

Figure 2 shows clearly that in symmetric zirconia the minimum of the total energy is found near the ideal c/a ratio and that the contour lines indicate only a small cross term between volume and c/a ratio, as expected for a cubic minimum. We would have preferred to include more points in the lower left-hand side of the plot, but numerical constraints made that too time consuming. The values used for the muffin-tin radii did not allow for smaller values of a or c, and a new set of calculations with a smaller value of these muffin-tin radii would be necessary. Nevertheless, the minimum is reasonably well described, since we have data points almost everywhere around it.

The data values were used to obtain a fit to the expression

$$\tilde{E}=E_0+\alpha(V-V_0)^2+\beta(V-V_0)(r-r_0)+\gamma(r-r_0)^2$$

and the resulting values are given in Table III. The quality of the second-order fit is good, and the rms error is 0.9 mRy. This is consistent with our estimated relative error of the data. The resulting value of the volume is 2% smaller than the experimental value, and such a deviation is normal for local-density calculations in which the volume is always underestimated by a few percent. In addition, the extrapolation of the experimental data to zero temperature introduces errors. The c/a ratio is within 1% of the ideal ratio, and therefore we can claim that with the oxygen atoms at the symmetric positions zirconia has a minimum total energy for a cubic structure consistent with the experimental value of the volume of the unit cell extrapolated to zero temperature.

TABLE III. Second-order parameters. Values of the parameters in the second-order fit to the total-energy data of Table II.

$E_0=-0.231$ Ry
$V_0=0.981$
$r_0=1.42$
$\alpha=3.52$ Ry
$\beta=0.471$ Ry
$\gamma=2.20$ Ry
$\epsilon_{\rm rms}=0.9$ mRy

The value of the total energy at the minimum is $-14\,980.231$ Ry for a unit cell containing six atoms. The systematic error in this number (due to incomplete convergence in the number of basis functions and the Brillouin-zone integration) is about 30 mRy. The total energy of the six atoms isolated in space is $-14\,976.44$ Ry and therefore the cohesive energy of zirconia with respect to neutral atoms is 3.92 Ry per six atoms. Including the uncertainty in the estimation of our systematic errors the value of the cohesive energy per formula unit is 1.96 ± 0.01 Ry. The experimental value is 1.68 Ry per formula unit. This is a standard difference in results of local-density calculations. It is related to an error in the atomic calculations, where multiplet corrections are ignored.[14] As a consequence, the total energy of an atom in local-density calculations is always too high, and the cohesive energy of a solid always too large. Typical discrepancies are on the order of 1 eV per atom, except in materials like NaCl where the cohesive energy is much closer to the experimental value[15] due to the simple structure of the Na and Cl atoms. For zirconia, we have an error in the cohesive energy of 0.09 Ry per atom, or 1.2 eV per atom, which is consistent with the general trends in local-density calculations.

The elastic constants are related to α, β, and γ in the following way:

$$\alpha=\frac{1}{2}\frac{\partial^2\tilde{E}}{\partial V^2}=\frac{1}{2}V_{\rm ref}\frac{1}{9V_0}[2(C_{11}+C_{12})+4C_{13}+C_{33}]\,,$$

$$\beta=\frac{\partial^2\tilde{E}}{\partial V\partial r}=V_{\rm ref}\frac{2}{9r_0}[C_{33}+C_{13}-(C_{12}+C_{11})]\,,$$

$$\gamma=\frac{1}{2}\frac{\partial^2\tilde{E}}{\partial r^2}=\frac{1}{2}V_{\rm ref}\frac{2V_0}{9r_0^2}[(C_{11}+C_{12})-4C_{13}+2C_{33}]\,,$$

and for a cubic system ($C_{11}=C_{33}$, $C_{12}=C_{13}$) the equations reduce to

$$\alpha_{\rm cubic}=\frac{1}{2}V_{\rm ref}\frac{C_{11}+2C_{12}}{3V_0}\,,$$

$$\beta_{\rm cubic}=0\,,$$

$$\gamma_{\rm cubic}=\frac{1}{2}V_{\rm ref}V_0\frac{C_{11}-C_{12}}{3}$$

as expected. The results derived from our total-energy data are $C_{11}+C_{12}=0.038$ a.u., $C_{13}=0.005$ a.u., and

TABLE IV. Second-order parameter without cross term. Values of the parameters in the second-order fit with $\beta=0$ to the total-energy data of Table II.

$E_0=-0.231$ Ry
$V_0=0.980$
$r_0=1.42$
$\alpha=3.46$ Ry
$\beta=0$ Ry
$\gamma=2.03$ Ry
$\epsilon_{\rm rms}=1.0$ mRy

$C_{33}=0.039$ a.u. Hence $C_{13}+C_{33}=0.044$ a.u. and this differs from $C_{11}+C_{12}$ by only 15%, which is about the error in the quoted values due to the uncertainty in the fitting procedure. The numerical errors in the elastic constants are about 10% and much larger than in other quantities, because in the calculation of these numbers one essentially has to take a second-order derivative of data with noise in one way or another.

Next we force a cubic fit by setting $\beta=0$, and we find the results shown in Table IV. The rms error is only slightly larger and consistent with the error in the data. In this case we find $C_{11}=0.034$ a.u. and $C_{12}=0.006$ a.u. These values are consistent with the data obtained without restrictions on β. In the remaining discussion we will use these data values and set $\beta=0$. The elastic constants are compared with experimental values in Table V. The orders of magnitude are correct, but a direct comparison is impossible because the experimental data are all for doped zirconia. Our calculated value for C_{11} is higher than the experimental one, which is a general trend in density-functional calculations. At the equilibrium volume the core repulsion and the ionic Coulomb attraction balance each other, but each of these forces is larger when the equilibrium volume is smaller. As a result, a smaller value of the equilibrium volume corresponds to a larger value of the bulk modulus and other elastic properties.

The second quantity density-functional calculations should give reliably is the charge density of a solid. Previous work[15] for NaCl has shown that we can indeed reproduce the experimentally measured form factors. There are no corresponding x-ray diffraction experiments for ZrO_2, and hence we can only draw a few conclusions. A typical charge-density map in a plane through four zirconium atoms (corners) and two oxygen atoms (center) is shown in Fig. 3. This figure shows that our choice for the muffin-tin radii is about right, since we capture most of the spherical regions inside the muffin-tin spheres. The minimal value of the charge density inbetween the two oxygen atoms is 0.027 a.u.$^{-3}$ which is slightly larger than what is expected for an ionic bond. The minimal value in between an oxygen and zirconium atom is 0.072 a.u.$^{-3}$, which is much larger than that found in ionic bonds. It is similar to the value of the charge density found in between the atoms in a metal and about one-third of the value found in diamond. The value of the charge density in between the zirconium atoms along the ⟨100⟩ direction is 0.027 a.u.$^{-3}$, while the corresponding value in the ⟨001⟩ direction is essentially zero. If one would hazard to make a prediction about covalent versus ionic nature of the bonds in symmetric zirconia, one definitely has to allow for some small amount of covalent bonding between zirconium and oxygen.

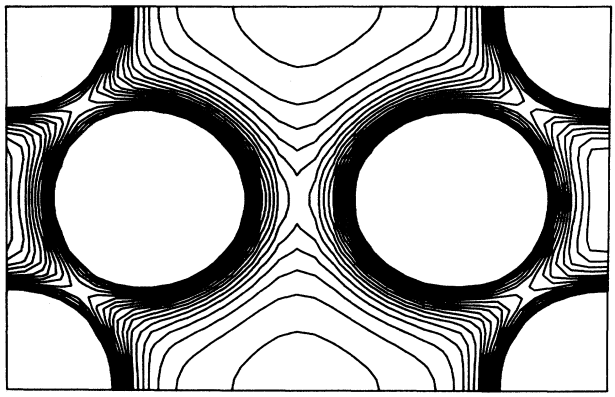

FIG. 3. Contours of equal charge density in a ⟨100⟩ plane through two oxygen (center) and four zirconium (corners) atoms.

The minimum in the charge density between the oxygen and zirconium atoms is about halfway between these atoms, and therefore one could say that the size of both atoms in zirconia is about 2.0 a.u. or 1.06 Å. These values indicate that the oxygen atoms are much smaller than its standard ionic radius would suggest, but that the zirconium atom is larger. The latter is mainly due to the "fat" $4p$ semicore electrons.

Figure 4 shows the $l=1$ component of the total charge inside the oxygen muffin-tin sphere as a function of the c/a ratio r and the relative volume. Since our sphere ra-

TABLE V. Elastic constants of cubic zirconia. Values of C_{11} and C_{12} for cubic zirconia in 10^{12} dyn/cm^2.

Temperature	Y_2O_3	Ref. No.	C_{11}	C_{12}
300	20%	16	3.91±0.03	1.20±0.05
300	15%	16	4.75	1.44
1000	15%	16	4.43	1.17
1700	15%	16	3.99	1.02
300	18%	17	3.75	0.75
300	8%	18	3.94	0.91
Theory	0%	5	2.22	0.61
Theory	0%	This work	5.0±1.0	0.9±0.2

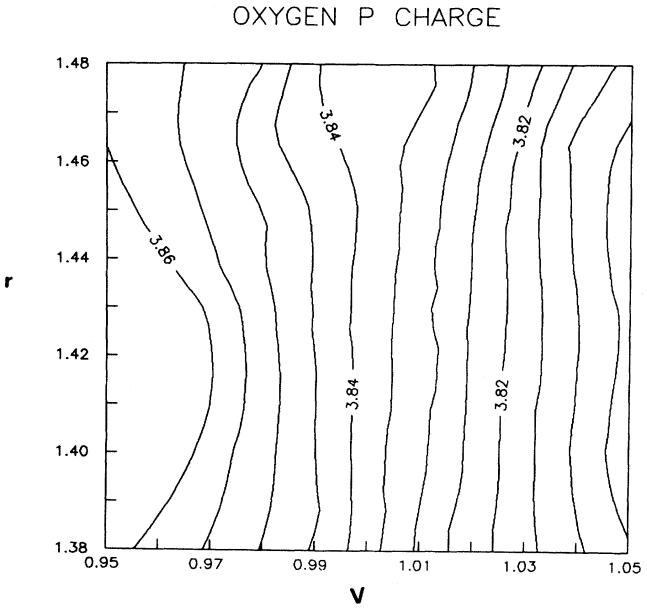

FIG. 4. Contours of equal total oxygen p charge within the oxygen muffin-tin sphere. Subsequent contour lines correspond to numbers of electrons which differ by 0.02 a.u.$^{-3}$.

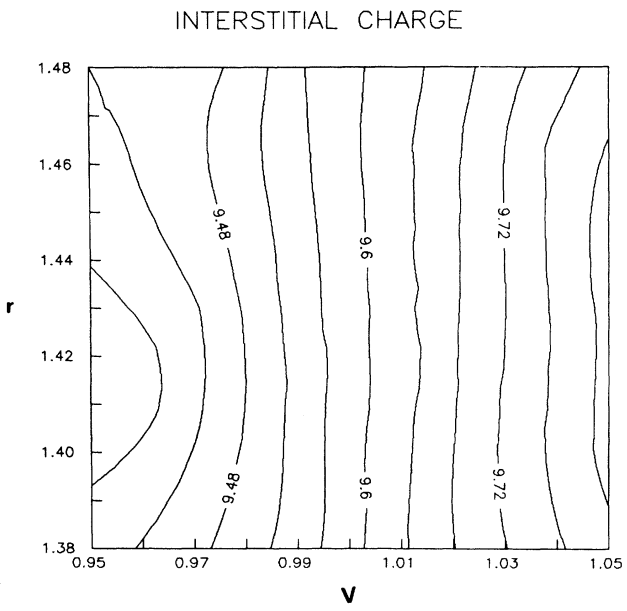

FIG. 5. Contours of equal interstitial charge. Subsequent contour lines correspond to numbers of electrons which differ by 0.04 a.u.$^{-3}$.

dius is smaller than the radius of the atom, not all p charge is included and some is found in what we label interstitial. In the central portion of the figure the charge density does only depend on V and not on c/a. The curvature of the contour lines at low and high values of the plot is due to the local fitting procedure and the lack of data in these regions. The charge inside the oxygen spheres decreases when the crystal expands, indicating that the oxygen atoms expand when the crystals expand. Therefore, at the equilibrium volume the oxygen atoms are under external pressure, which explains their small ionic radius. Figure 5 shows the total charge in the interstitial region as a function of r and V, and this charge increases with increasing volume, as expected. The interstitial charge density is increasing by a larger amount than can be accounted for by the oxygen atoms: the zirconium atoms are also expanding when the volume increases.

The electric-field gradient at the nuclear sites is a quantity which can be derived directly from the charge densities in our calculations. Numerically, one expands the Coulomb potential near a nucleus in the form

$$rV_C(\mathbf{r}) = \sum_{l,m} V_{lm}(r) Y_{lm}(\hat{\mathbf{r}})$$

and the multipole moments are defined by

$$q_{lm} = \lim_{r \downarrow 0} r^{-l-1} V_{lm}(r) \ .$$

Restrictions are present due to symmetry and up to second order the expansions for the Coulomb potential are

$$q_0 \frac{1}{\sqrt{4\pi}} + q_2 \frac{\sqrt{5}}{2\sqrt{4\pi}}(3z^2 - r^2)$$

near Zr and

$$q_0' \frac{1}{\sqrt{4\pi}} + q_1' \frac{\sqrt{3}}{\sqrt{4\pi}} z + q_2' \frac{\sqrt{5}}{2\sqrt{4\pi}}(3z^2 - r^2) + q_2'' \frac{\sqrt{5}}{2\sqrt{4\pi}}(x^2 - y^2)\sqrt{3}$$

near 0, where the coordinates are chosen according to Fig. 1.

Since we do not allow for nonspherical distortions of the inner core electrons our calculated values cannot be compared directly with experiment, but have to be corrected for the polarization of the inner core electrons. This is discussed in the next section. Figure 6 shows the electric-field gradient at a zirconium site, while Fig. 7 gives the electric-field gradient at an oxygen site. In both cases, the values of the electric-field gradient only depend on the c/a ratio and not on volume, which is to be expected. Also, we find a zero value of the field gradients for a c/a ratio close to the ideal value of 1.414. The small deviation is due to the fact that the value of the parameter d_z is 0.01 instead of exactly zero. These figures show that our calculated field gradients are consistent for different geometries and that the relative errors in these field gradients are small.

Another quantity related to the charge density is the average Coulomb potential in the unit cell. This value is useful when comparing different calculations, since the positions of the energy bands can be scaled with respect to this parameter. In general, in an infinite solid the zero of energy is not defined. In the FLAPW method this zero is set in a numerically convenient but physically arbitrary way. Therefore the value of the average Coulomb poten-

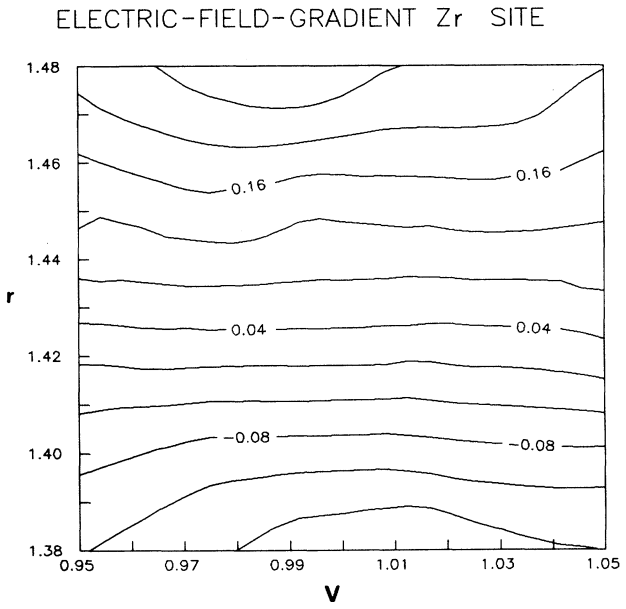

FIG. 6. Electric-field gradient q_2 at a zirconium site.

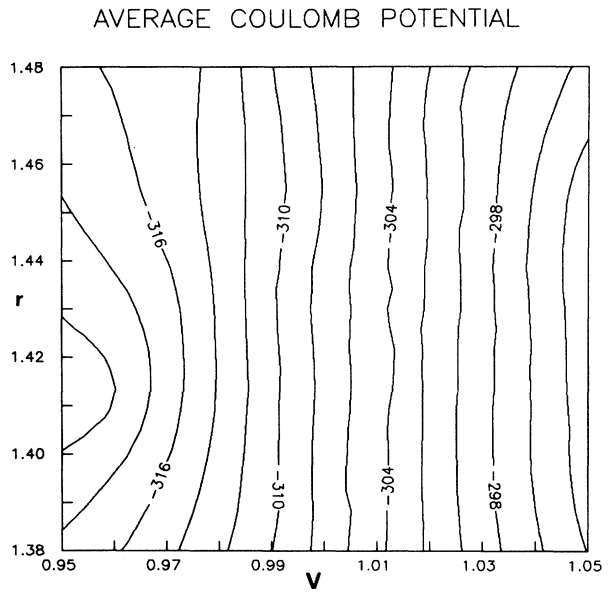

FIG. 8. Average Coulomb potential in the unit cell.

tial in the unit cell is model dependent, but is a good reference for values of the energy bands and related quantities. The values shown in Fig. 8 range from -0.321 to -0.289 Ry and they do only depend on the volume of the unit cell. These changes are related to the expansion of the constituent atoms when the unit cell volume increases.

The energy eigenvalues obtained when solving the Kohn-Sham equations should not be related directly to excitation energies. There is only a correspondence in first order, and the error can be large when the nature of the electronic states changes considerably. For example, the band gap in semiconductors derived from these energy eigenvalues is always much too small, with differences on the order of 30%. The changes in these numbers as a function of the geometry have smaller errors associated with them because systematic errors do cancel. In Fig. 9 we present the width of the valence band of zirconia derived from these energy eigenvalues as a function of volume and c/a ratio, and in Fig. 10 the value of the gap between the valence and the conduction band. The width of the valence band ranges from 390 to 450 mRy, while

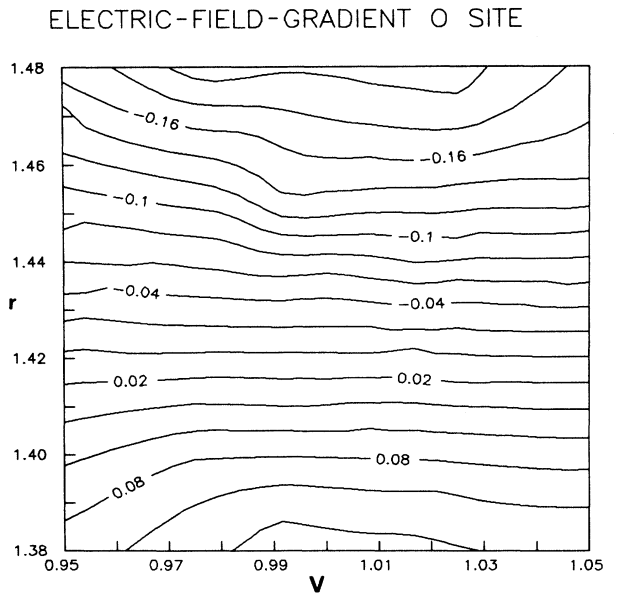

FIG. 7. Electric-field gradient q_2' at an oxygen site.

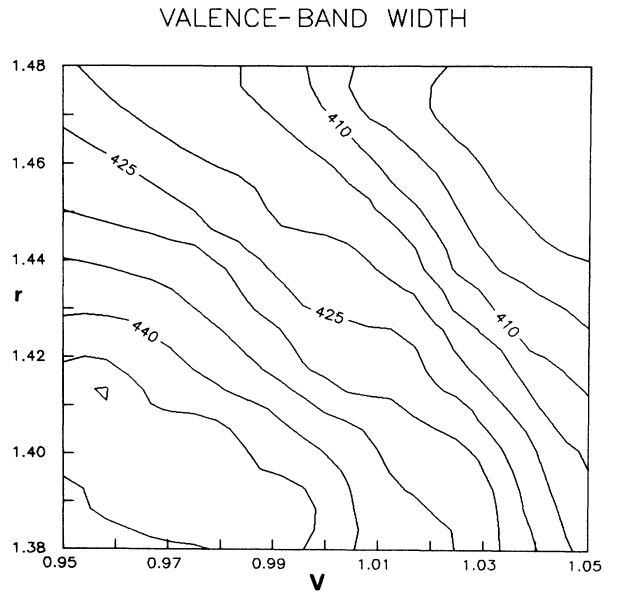

FIG. 9. Kohn-Sham valence-band width.

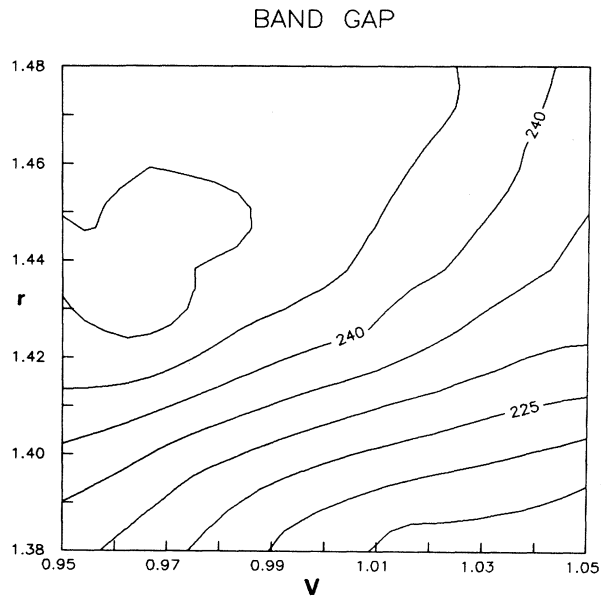

FIG. 10. Kohn-Sham band gap.

the gap varies between 250 and 210 mRy. The pattern of these changes has no simple dependence on volume or c/a ratio, and the nature of the geometry of the local bonds plays a dominant role.

V. TETRAGONAL ZIRCONIA

We have studied the effect of a displacement of the oxygen atoms parallel to the z axis for a number of values of a and c. We always stayed within the space group D_{4h}^{15}, as dictated by experiments. In a point-charge model the total energy is lowest for $d_z=0.25$ and the CaF_2 structure is unstable. The soft atomic cores on the other hand stabilize the cubic structure when the density of the atoms is sufficiently high. It is therefore of interest to investigate for which values of a and c a structural instability occurs in ZrO_2.

Table VI presents the total energy as a function of d_z for several values of a and c. We have interpolated these data by the function

$$E=E_0+E_2d_z^2+E_4d_z^4$$

and plotted these functions in Fig. 11. The parameters E_i are given in Table VII. An instability is clearly seen for all data sets except C. It is also evident that the instability becomes more pronounced at larger values of a and c. This is to be expected, since the core repulsion is not very strong at large separations of the atoms. In that case the long-range Coulomb forces will pull the zirconium and oxygen atoms together as close as possible.

The behavior as a function of a and c can be studied by expanding E_2 and E_4 as a function of a and c,

$$E_i=\alpha_i+\beta_i a+\gamma_i c\ .$$

The results are given in Table VIII. The rms errors are very large, indicating that these fits only have qualitative meaning. The lattice instability is related to the sign of E_2. If E_2 is negative, the total energy is a maximum near $d_z=0$ and the CaF_2 structure is unstable. If E_2 is positive, it is stable. E_4 should always be positive in order that our simple formula makes sense. The line $E_4=0$ is given by $c=54.14-6.03a$ and is far outside the region of interest. The line $E_2=0$ is given by $c=13.38-0.62a$ and crosses the lower left corner of the region in which we have plotted our total-energy data (Fig. 2). Since the

TABLE VI. Total energy of tetragonal zirconia. Calculated total energy per unit cell of tetragonal zirconia as a function of the displacement d_z of the oxygen atoms, in mRy. The integer part $-14\,980$ Ry has to be added to these numbers to get the complete value of the total energy.

	a (a.u.)	c (a.u.)	d_z	Energy (mRy)
Data set A	6.88	9.96	0.010	−206
	6.88	9.96	0.032	−214
	6.88	9.96	0.065	−212
	6.88	9.96	0.100	−150
Data set B	6.95	9.73	0.010	−211
	6.95	9.73	0.032	−215
	6.95	9.73	0.065	−209
Data set C	6.70	9.58	0.01	−231
	6.70	9.58	0.04	−228
	6.70	9.58	0.07	−190
Data set D	6.64	9.84	0.01	−223
	6.64	9.84	0.04	−226
	6.64	9.84	0.07	−193
Data set E	6.88	9.52	0.01	−224
	6.88	9.52	0.04	−226
	6.88	9.52	0.07	−203

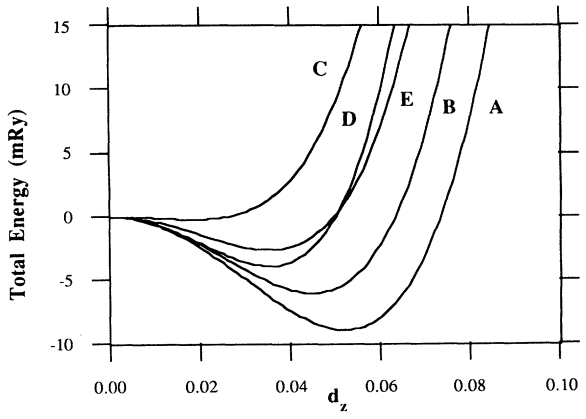

FIG. 11. Total energy (in mRy) per unit cell as a function of d_z. All curves are scaled to zero for $d_z=0$.

minimum at the total energy also occurs in this region one can expect that a tetragonal distortion will be present.

Including the dependence of the total energy on d_z leads to the following interpolation for the total energy $\tilde{E}$ as a function of a, c, and d_z:

$$\tilde{E}(a,c,d_z)=E_0+\alpha(V-V_0)^2+\gamma(r-r_0)^2 -E_2(a,c)0.01^2-E_4(a,c)0.01^4 +E_2(a,c)d_z^2+E_4(a,c)d_z^4 .$$

Minimizing this expression gives the following values for tetragonal zirconia: $V=0.985$, $r=1.425$, $d_z=0.029$, and $\Delta E=-1.3$ mRy for two formula units, where ΔE is the difference in energy between the cubic minimum and the tetragonal minimum. This indicates that at zero temperature our electronic structure calculations indeed predict that zirconia is tetragonally distorted.

A typical charge-density map of tetragonal zirconia is shown in Fig. 12. Half of the zirconium-oxygen bonds have become stronger and the other half weaker compared with the bonds in symmetric zirconia. The minimum value of the density between oxygen atoms (in point *A*) is unchanged (0.027 a.u.$^{-3}$), the value for the weak zirconium-oxygen bond (in point *B*) is now 0.041 a.u.$^{-3}$ (down from 0.072 a.u.$^{-3}$), and the value in the strong zirconium-oxygen bond (point *C*) is now 0.120 a.u.$^{-3}$ This last value is half that found in diamond. A big difference with diamond is, of course, the lack of directional bonding closer to the oxygen nucleus. The oxygen 2*s* and 2*p* bands are still clearly separated and no hybrid bonding states are formed. The main reason for the increase in charge density between zirconium and oxygen is the smaller distance between the atoms, causing a larger overlap of the atomic spheres. The softness of the atomic spheres is important here, hard spheres would not allow any overlap. Another consequence of the displacement of the oxygen atoms is the increase in charge density between the zirconium atoms in the ⟨100⟩ direction, which makes the bonds in this direction stronger and causes the tetragonal distortion of the whole unit cell.

We have also calculated the electric-field gradients as a function of d_z and the results are shown in Fig. 13 for the zirconium sites (q_2) and in Fig. 14 for the oxygen sites (q_2'). These field gradients are not exactly zero at $d_z=0$, because the c/a ratio is not exactly $\sqrt{2}$. One sees immediately that the electric-field gradients at the zirconium sites are much larger than those at the oxygen sites. Also, at the zirconium sites the main contribution is due to the fact that d_z is nonzero, while at the oxygen sites the effects of the tetragonal distortion of the zirconium atoms is equally important as the change in the positions of the oxygen atoms.

The numerical values for the electric-field gradients cannot be compared directly with experiment, since no data are available. Measurements have been performed, however, for Hf nuclei in zirconia.[19] Since hafnium is similar to zirconium, no large changes in electronic structure are expected After neutron activation, the hafnium nucleus decays into a tantalum nucleus, which relaxes into its ground state by emitting two γ rays. Perturbed angular correlation[19] experiments using these γ rays yield information about the field gradient near a tantalum atom on a zirconium site. The measured value for q_2 is 3.51 Ry a.u.$^{-2}$, while our calculated values for $d_z=0.060$ (which is the experimental value) is around 1.25 Ry a.u.$^{-2}$. The difference is due to the effects of the core electrons, which respond differently in tantalum and zirconium. The Sternheimer antishielding factors γ_∞ are -28 for zirconium and -61 for tantalum. In a point charge model calculated field gradients are multiplied by a factor $(1-\gamma_\infty)$, indicating that changes in the tantalum core electrons amplify field gradients more, the ratio being about 2.1. Taking this effect into account we would predict a value for q_2 for tantalum in zirconia of about 2.7 Ry a.u.$^{-2}$, which is about 20% smaller than the experimental value. Finally, after the hafnium nucleus decays to a tantalum nucleus the life time before emitting

TABLE VII. Parameters E_i for energy distortion. This table gives the parameters E_i in the expression $E=E_0+E_2d_z^2+E_4d_z^4$ for the total energy of tetragonal zirconia as a function of the displacement d_z of the oxygen atoms. The column $d_{z,\min}$ denotes the value of d_z for which this energy is minimal, and ΔE gives the energy difference in mRy between the minimal value and the value for $d_z=0$.

	a (a.u.)	c (a.u.)	E_0 (mRy)	E_2 (mRy)	E_4 (mRy)	$d_{z,\min}$	ΔE (mRy)
A	6.88	9.96	−207	-6.61×10^3	1.23×10^6	0.052	8
B	6.95	9.73	−210	-6.02×10^3	1.50×10^6	0.044	6
C	6.70	9.58	−231	-1.37×10^3	1.98×10^6	0.019	0
D	6.64	9.84	−222	-6.26×10^3	2.50×10^6	0.035	4
E	6.88	9.52	−224	-4.27×10^3	1.73×10^6	0.035	2

TABLE VIII. Parametrization of E_2 and E_4. The parameters E_i are expanded as a linear function of a and c according to $E_i=\alpha_i+\beta_i a+\gamma_i c$. The values of the parameters α_i, β_i, γ_i, and the rms error $\delta_{\rm rms}$ are in mRy.

	α_i	β_i	γ_i	$\delta_{\rm rms}$
E_2	123×10^3	-5.66×10^3	-9.19×10^3	1.1×10^3
E_4	28.8×10^6	-3.21×10^6	-0.532×10^6	0.19×10^6

the first photon is 18 μsec, which is sufficiently large to cause a deformation of the lattice near the impurity, which increases the field gradients. Since our value corrected for the difference in shielding is still too small compared with experiment, we conclude that this local distortion is likely to be present.

VI. TETRAGONAL-TO-CUBIC PHASE TRANSITION

So far we have only discussed properties at zero temperature. Our results indicate that tetragonal zirconia has a lower total energy than cubic zirconia, consistent with experiment. Also, the values of the volume of the unit cell we obtained in our calculations are close to the experimental values extrapolated to zero temperature. The value of the c/a ratio we found, 1.425, is a 0.8% deviation from the ideal value. The experimental value extrapolated to zero temperature, on the other hand, is about 1.45% and 2.5% larger than the ideal value. The experimental value of d_z extrapolated to zero temperature is about 0.055 and is much larger than our value of 0.029. Hence the degree of the tetragonal distortion predicted by our results is smaller than found experimentally, although the linear extrapolation might also be a problem for the lower temperatures.

Phonons play an important role at higher temperatures. For values of the temperature much higher than the Debye temperature, the Grüneisen parameter γ of zirconia is a constant and as a result the coefficient of thermal expansion α is also a constant (ignoring the temperature dependence of the bulk modulus B). They are related by

$$\alpha=\frac{1}{3V}\left[\frac{\partial V}{\partial T}\right]_P=\frac{\gamma c_v}{3B} \quad \text{with } B=\tfrac{1}{3}(C_{11}+2C_{12}) .$$

From Ref. 13 we find that $\alpha=12\times10^{-6}$ K^{-1} for the range in temperature from 1160 °C to 1925 °C. At these high temperatures we can replace c_v by $3Nk/V_{\rm ave}$, with $N=6$ and $V_{\rm ave}=477$ a.u.[3] Our values for the elastic constants indicate that $B=0.015$ a.u. and hence we find $\gamma=2.3$. This value is somewhat larger than the high-temperature value for the alkali halides, but much larger than the value of $\frac{1}{3}$ found in a Debye model. The experimental values for the **k**-dependent Grüneisen parameter at Γ in Ref. 18 are about twice as large. This indicates that there are large variations of the Grüneisen parameter as a function of **k**. Calculations of the phonon spectrum are needed in order to further investigate the Grüneisen parameter from a theoretical point of view.

In our next step we assume that the phonons are responsible for determining the value of the volume at a given temperature. Hence the relative volume increases linearly from 1.060 at 1160 °C to 1.089 at 1925 °C. At each value of the temperature we fix the value of the relative volume according to this linear interpolation and then minimize the electronic energy to find the tetragonal distortion and the internal displacement of the oxygen atoms. Following this procedure we find that both the value of $r/\sqrt{2}$ (Fig. 15) and d_z (Fig. 16) are linear functions of the temperature. In Fig. 15 we plot the quantity $r/\sqrt{2}$, because that gives a better indication of the deviation from cubic symmetry. In these figures we have also included experimental results from Ref. 13. The temper-

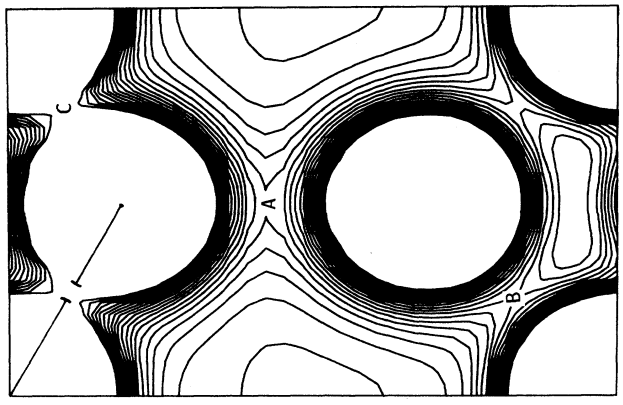

FIG. 12. Contours of equal charge density in a ⟨100⟩ plane through two oxygen (center) and four zirconium (corners) atoms for a tetragonal zirconia.

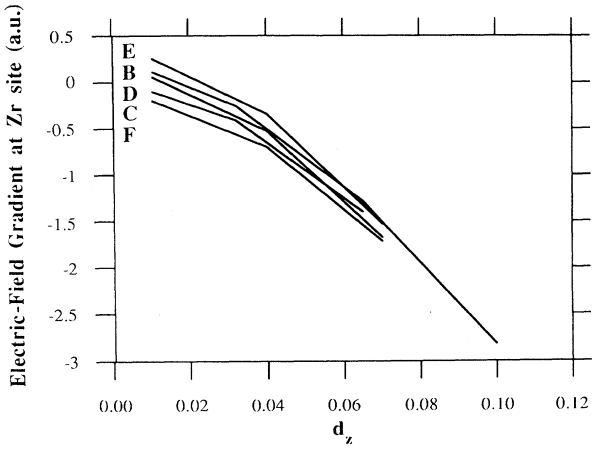

FIG. 13. Electric-field gradient q_2 at a zirconium site as a function of d_z.

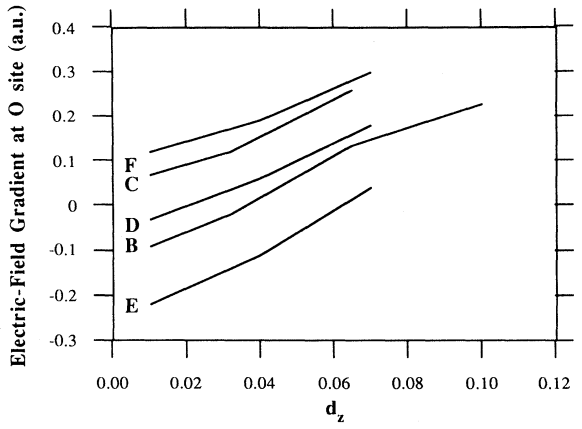

FIG. 14. Electric-field gradient q_2' at an oxygen site as a function of d_z.

ature scale in these figures is derived from the experimental values of the volume as a function of temperature. The discrepancy between experiment and theory for r is larger than for d_z, which is not surprising since a tetragonal distortion of the whole unit cell will affect the phonon spectrum. In general we can conclude that the tetragonal distortion is larger at elevated temperatures because of the volume expansion due to thermal excitation of phonons.

In Fig. 17 we present the difference in energy between the tetragonal phase and the cubic phase ($r=\sqrt{2}$, $d_z=0$) at the same volume as a function of temperature. We find that the energy difference increases as a function of temperature. In that sense tetragonal zirconia becomes more stable at high temperature. The difference in energy is mainly due to the change in the value of d_z. This parameter describes an optical phonon at Γ. The thermal energy per unit cell associated with all phonons pertaining to d_z, i.e., phonons for all values of $\mathbf{k}$ in the first Brillouin

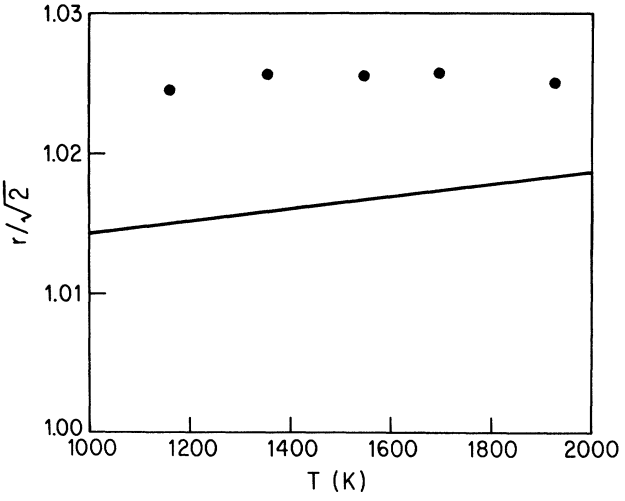

FIG. 15. Tetragonal distortion $r/\sqrt{2}$ as a function of temperature. Experimental values are indicated by dots.

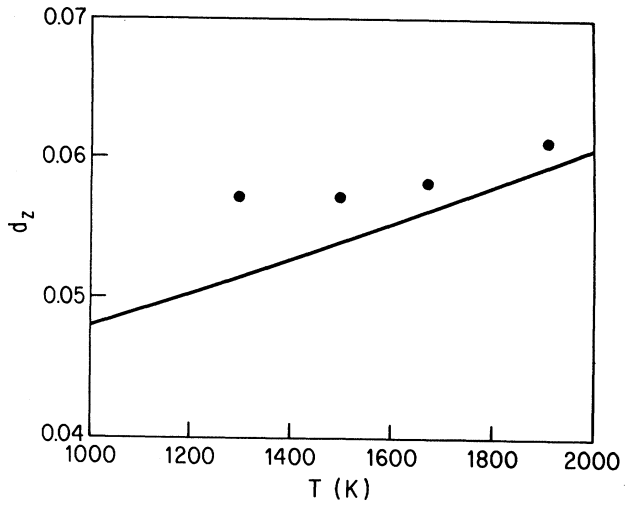

FIG. 16. Internal oxygen displacement of d_z as a function of temperature. Experimental values are indicated by dots.

zone, is just kT. The straight line in Fig. 17 is $E=-kT$, and a comparison between the two curves shows that the thermal energy is almost the same as the energy difference between tetragonal and cubic zirconia.

The total energy of the tetragonal phase is lower than that of the cubic phase, and hence a stabilization of cubic zirconia at elevated temperatures has to involve a difference in entropy. One explanation of the stability of cubic zirconia at higher temperatures is based on a mechanism that relies on the presence of oxygen defects. This is a plausible explanation, but based on our total-energy data we cannot exclude the possibility that the tetragonal-to-cubic phase transition is driven by phonons. A detailed calculation of the phonon spectrum is needed to decide if the entropy contribution due to the phonons is sufficient to stabilize cubic zirconia. The entropy related to the d_z phonons in cubic zirconia is certainly larger than that in tetragonal zirconia, since in the former there

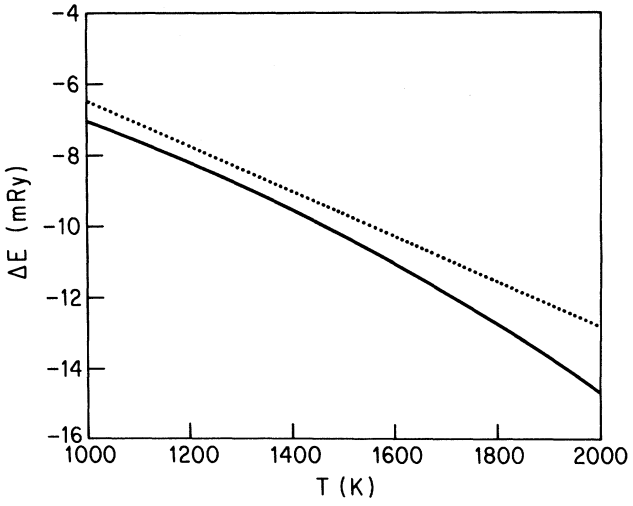

FIG. 17. Energy difference (mRy) per unit cell between tetragonal and cubic zirconia as a function of temperature. The straight line corresponds to $E=-kT$.

are three possible choices for the orientation of the tetragonal distortion. As a consequence, the number of phonons is increased.

VII. SUMMARY

In this paper we have investigated the electronic structure of cubic and tetragonal zirconia. Our total-energy data indicate that at zero temperature tetragonal zirconia will be more stable than cubic zirconia. The elastic properties of cubic zirconia are consistent with experimental data, but a direct comparison is impossible because measurements are always performed on samples containing Y_2O_3. The values of the electric-field gradient are also consistent with experiment. If we use the experimentally determined values of the unit-cell volume as a measure of the temperature we find a qualitative agreement between calculated and experimental structural parameters. We conclude that the structure of tetragonal zirconia can be derived from density-functional calculations without the need of introducing defects or vacancies.

Our calculations do not directly address the problem of stabilizing cubic zirconia, since we are not able to evaluate the entropy. Our total-energy data are, however, very useful as input for more detailed thermodynamical calculations. Model potentials in such an approach will have to follow the trends in total energy we have discussed in this paper. Simple arguments based on the total-energy data show that the contribution to the free energy of optical phonons related to the displacement of the oxygen atoms is of the same order of magnitude as the energy difference between cubic and tetragonal zirconia. Whether this contribution is sufficient to stabilize cubic zirconia has to be investigated in thermodynamical calculations.

ACKNOWLEDGMENTS

This research was supported by the U.S. Department of Energy (DOE) under Grant No. DE-FG06-88ER45352. The computations were performed at the National Magnetic Energy Fusion Center with computer time made available by DOE. We would like to thank Professor J. A. Gardner for many helpful and stimulating discussions.

[1]W. Nernst, Z. Electrochem. **6**, 41 (1990).

[2]See, for example, E. C. Subbarao, in *Science and Technology Zirconia,* edited by A. H. Heuer and L. W. Hobbs, Advances in Ceramics Vol. 3 (The American Ceramic Society, Columbus, OH, 1981).

[3]S. M. Ho, Mater. Sci. Eng. **54**, 23 (1982).

[4]M. Morinaga, H. Adachi, and M. Tsukuda, J. Phys. Chem. Solids **44**, 301 (1983).

[5]L. L. Boyer and B. M. Klein, J. Am. Ceram. Soc. **68**, 278 (1985).

[6]Proceedings of the International Conference on Electronic Structure and Phase Stability in Advanced Ceramics, Argonne, IL, 1987 [Physica B **150**, 1 (1988)].

[7]H. J. F. Jansen and J. A. Gardner, Physica B **150**, 10 (1988)

[8]See, for example, *Theory of Inhomogeneous Electron Gas,* edited by S. Lundqvist and N. H. March (Plenum, New York, 1983).

[9]U. von Barth and L. Hedin, J. Phys. C **5**, 1629 (1972); J. F. Janak, Solid State Commun. **25**, 53 (1978).

[10]See, for example, V. L. Moruzzi, J. F. Janak, and A. R. Williams, *Calculated Electronic Properties of Metals* (Pergamon, New York, 1978).

[11]H. J. F. Jansen and A. J. Freeman, Phys. Rev. B **30**, 561 (1984).

[12]D. Singh and H. Krakauer, Bull. Am. Phys. Soc. **35**, 418 (1990).

[13]P. Aldebert and J. P. Traverse, J. Am. Ceram. Soc. **68**, 34 (1985).

[14]R. E. Watson *et al.*, Bull. Am. Phys. Soc. **35**, 309 (1990).

[15]H. J. F. Jansen and A. J. Freeman, Phys. Rev. B **33**, 8629 (1986).

[16]D. W. Liu, C. H. Perry, A. A. Feinberg, and R. Currat, Phys. Rev. B **36**, 9212 (1987).

[17]S. Shin and M. Ishigame, Phys. Rev. B **34**, 8875 (1986).

[18]T. Hailing and G. A. Saunders, J. Mater. Sci. Lett. **1**, 416 (1982).

[19]H. Jaeger *et al.*, J. Am. Ceram. Soc. **69**, 458 (1986).